



An experimental study of the synergistic effects of BMIM-BF₄, BMIM-DCA and TEACl aqueous solutions on methane hydrate formation

Ali Rasoolzadeh¹ · Jafar Javanmardi¹ · Amir H. Mohammadi^{2,3}

Received: 14 April 2018 / Published online: 13 March 2019
© The Author(s) 2019

Abstract

In this work, the effects of three ionic liquids (ILs), namely, 1-butyl-3-methylimidazolium tetrafluoroborate, 1-butyl-3-methylimidazolium dicyanamide and tetraethyl-ammonium chloride, on methane hydrate formation and dissociation kinetic parameters were studied. The kinetic parameters including the initial rate of hydrate formation, hydrate stability at atmospheric pressure and hydrate storage capacity were evaluated. The experimental measurements were performed in an initial pressure range of 3.5–7.1 MPa. It was found that both of ILs with imidazolium-based cation increase the initial methane hydrate formation rate while the IL with ammonium-based cation leads to a decrease in the initial methane hydrate formation rate. It was also interpreted from the results that all of the three studied ILs decrease methane hydrate stability at atmospheric pressure and increase methane hydrate storage capacity. Finally, both of ILs with imidazolium-based cations were found to have higher impacts on decreasing hydrate stability at atmospheric pressure and increasing the methane hydrate storage capacity than the applied IL with ammonium-based cation.

Keywords Storage capacity · Gas hydrate · Initial rate · Ionic liquids · Natural gas

List of symbols

n_{total}^0	Initial total moles of gas in the system
n_{cell}	Moles of gas in the cell at time t
n_f	Moles of gas in the junctions at time t
n_h^t	Moles of gas in the hydrate at time t
R	The universal gas constant
P	The pressure of system
T_a	The ambient temperature
T_{cell}	The cell temperature
V_{cell}	The cell volume
V_f	The junction volume

Z_a	Methane compressibility factor at ambient temperature
Z_{cell}	Methane compressibility factor at cell temperature

1 Introduction

Gas hydrates, or clathrate hydrates, are crystal-like solid compounds similar to ice or snow, in which small molecules of gases and/or some volatile liquids with appropriate dimensions (guest molecules) are entrapped in the empty cages made by the water molecules (host molecules) through hydrogen bonds. The guest molecules, called “hydrate formers,” make the unstable hydrate structures stable. By taking into account the nature, dimension and type of the hydrate formers, three usual structures of I, II and H can be formed (Carroll 2002, 2009).

Gas hydrates have been the subject of many scientific studies over the past century (Sloan and Koh 2008). Hammerschmidt (1934) stated that gas hydrates may cause petroleum pipeline blockages, which can lead to economic losses and process failure. Since then, gas hydrates became an unfavorable phenomenon and several methods are used to avoid their formation in the pipelines, such as heating,

Edited by Xiu-Qin Zhu

✉ Jafar Javanmardi
Javanmardi@sutech.ac.ir

¹ Department of Chemical Engineering, Shiraz University of Technology, Shiraz, Iran

² Institut de Recherche en Genie Chimique et Petrolier (IRGCP), Paris Cedex, France

³ Discipline of Chemical Engineering, School of Engineering, University of KwaZulu-Natal, Howard College Campus, King George V Avenue, Durban 4041, South Africa

pressure reduction, water elimination and adding inhibitors. The latter method is one of the most used ways employed in industry (Karaaslan and Parlaktuna 2002; Koh et al. 2002; Lederhos et al. 1996).

Since the middle of 1960s, scientists have been attracted to investigate the applications of gas hydrates. Although gas hydrates have the disadvantage of plugging the pipelines, they have various applications. Gas hydrates are potentially great resources of natural gas (Sloan and Koh 2008; Sloan 2003), they can be utilized as a medium for storage and transportation of gas (Koh et al. 2011; Javanmardi et al. 2005; Sun et al. 2003), they can be used as a new method in the separation of gases (Uchida et al. 2005; Kang et al. 2001; Sugahara et al. 2005; Zhang et al. 2009) and a new method for CO₂ capturing (Kang et al. 2001; Li et al. 2005; Seo and Kang 2010), etc.

Ionic liquids (ILs) are salts that are liquid at temperatures below 100 °C. They have very low vapor pressures and are green solvents (green solvents are environmentally friendly solvents, which can be used as an alternative of petrochemical solvents) which do not decompose even at extra high temperatures. Ordinary ILs may be composed of asymmetric organic cations like imidazolium, ammonium, pyrrolidinium, etc., with alkyl chain and anions like halide ions, tetrafluoroborate, dicyanamide, nitrate, etc. (Wasserscheid and Welton 2008).

Several scientists have investigated the formation and dissociation of gas hydrate kinetics in the presence of ILs. Xiao and Adidharma (2009) were the first scientists who used five ILs with imidazolium-based cations as a new class of hydrate inhibitors called “dual-function” inhibitors. Xiao et al. (2010) studied the impacts of six ILs with imidazolium-based cations on methane hydrate equilibrium curves, nucleation rate and growth rate and observed that they had inhibition effects. Del Villano and Kelland (2010) studied the effects of two ILs with imidazolium-based cations on structure II gas hydrates, and they claimed that the two ILs with imidazolium-based cation had a poor kinetic inhibition effect on hydrate formation. Kim et al. (2011) investigated the impact of ILs with pyrrolidinium-based cations on methane hydrate formation, and they observed both thermodynamic and kinetic inhibition effects of ILs. Nazari et al. (2013) studied thermodynamic and kinetic effects of three ILs with imidazolium-based cations on methane hydrate formation. They also presented kinetic modeling of methane hydrate inhibition on the basis of IL nature and electrostatic intermolecular interactions between water and ILs (Nazari et al. 2013). Kang et al. (2013) applied a mixture of ILs and polymer inhibitors and observed a synergistic effect on methane hydrate inhibition. Richard and Adidharma (2013) studied the performance of ILs with imidazolium-based cations and their mixtures with conventional inhibitors on methane hydrate formation. Tariq et al. (2014) performed a

full review on the role of ILs in thermodynamic and kinetic inhibition of gas hydrates. Zare et al. (2015) investigated the effect of ILs with imidazolium-based cations and their mixtures with ethylene glycol monoethyl ether on methane hydrate induction time, methane consumption and temperature. Kang et al. (2016) observed the synergistic inhibition effect of ILs on gas hydrate formation when mixed with a common kinetic inhibitor like polyvinylcaprolactam (PVCap). Rasoolzadeh et al. (2016) measured methane hydrate formation induction time in the presence of different ILs and developed a semiempirical relation for induction time modeling. Lee et al. (2016a, b, c) proved that HEMM-Cl acts as a kinetic hydrate promoter and HEMM-BF₄ acts as a kinetic hydrate inhibitor for methane hydrate formation. Qureshi et al. (2016) performed an experimental study of the thermodynamic and kinetic inhibition effects of ILs with synergistic compounds on gas mixtures. Lee et al. (2016a, b, c) performed an experimental study of thermodynamic and kinetic inhibition effects of various ILs and their mixtures with PVCap on methane hydrate formation. Lee et al. (2016a, b, c) evaluated the synergetic inhibition effects of some ILs on the kinetic inhibition performance of PVCap on natural gas hydrate formation.

For gas storage and transport using hydrate media, several variables, such as the initial rate of hydrate formation, hydrate stability at atmospheric pressure and hydrate storage capacity, are key parameters (Sloan and Koh 2008). Gas hydrate technology has some advantages. For example, it has low energy consumption, it is clean, it is safe, etc., but some obstacles also exist like the slow rate of hydrate formation and hydrate stability issues (Sloan and Koh 2008). It has been proved that 1 m³ of hydrate can store about 180 m³ of gas at standard conditions when all the hydrate cages are completely filled (Sloan and Koh 2008), but in practical studies, this value is much less than 180 m³ (Sloan and Koh 2008). Therefore, several additives have been used to enhance these parameters of hydrate formation (Sloan and Koh 2008).

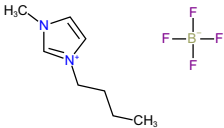
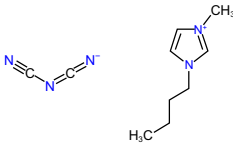
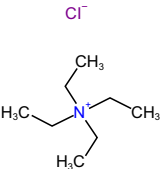
The purpose of this work was to investigate experimentally the effects of three ILs, namely, (BMIM-BF₄), (BMIM-DCA) and (TEACl), on the initial rate of hydrate formation, hydrate stability at atmospheric pressure and hydrate storage capacity for the case of methane hydrate. The results are presented in the following sections.

2 Experimental section

2.1 Materials

Table 1 indicates the specifications, suppliers and purities of the ILs utilized in the experiments. The hydrate former used in this work was methane having a mole purity of 99.95%,

Table 1 Specifications, suppliers and purities of ILs

Symbol	Chemical formula	Molar mass, g mol ⁻¹	Solubility g L ⁻¹	Density at 20 °C, g cm ⁻³	Supplier	Purity, %	Chemical structure
BMIM-BF ₄	C ₈ H ₁₅ BF ₄ N ₂	160.95	Soluble	1.18	Merck	99	
BMIM-DCA	C ₁₀ H ₁₅ N ₅	205.26	Soluble	1.06	Merck	99	
TEACl	(C ₂ H ₅) ₄ N(Cl)	183.73	1410	Solid	Merck	98	

purchased from Air Products Company. The deionized water was provided in our laboratory. The ILs aqueous solutions were prepared by using a gravitational method with the accuracy of 0.01 weight percent (0.0001 mass fraction). An electronic A&D balance (HR-200 laboratory balance, Japan) with a capacity of 210 g was used for this purpose.

2.2 Apparatus

The heart of the experimental setup is the stainless steel (SS-316) reactor/cell having a total volume of 90 cm³. The reactor can withstand the pressures up to 15 MPa. For measuring the temperature of the reactor, a high precision thermometer (Pt-100, OMEGA Company, UK) with a precision of ± 0.1 K is linked to the reactor. Pressure measurement inside the reactor is conducted by a pressure transducer (P-2, Validyne Company, USA) which is connected to the reactor with an uncertainty of 0.25% of the full scale. The reactor is put in an ethanol cooling bath. The adjustment of the temperature is obtained by applying a controllable circulator (TCS-1) which is capable of programming (Julabo FP-50, Germany). Figure 1 demonstrates the overview of the experimental setup.

2.3 Procedure

2.3.1 Hydrate formation rate

Deionized water was used to wash the reactor; then, the reactor was dried thoroughly. 20 cm³ of IL aqueous solution

or pure water was fed into the reactor at the start of each experiment. The reactor was filled with methane to reach the studied pressure at 298.15 K. After keeping the system at 298.15 K for 1 h to eliminate the hydrate memory effect for each experiment, the system was quickly cooled down to 287.15 K and kept at constant temperature for 1 h to reach the “equilibrium conditions,” i.e., giving enough time to the system to reach thermal equilibrium and transferring different species to each phase to reach the equilibrium conditions. The agitation was started at a rate of 1000 rpm at the beginning of the experiment. After achieving the equilibrium conditions at 287.15 K, the system was cooled down again to 272.65 K at the slow rate of 1 K h⁻¹ and kept at 272.65 K for 15 h to guarantee the completion of gas hydrate formation. The time, pressure, system temperature and ambient temperature were recorded during the entire experiment. The amount of gas in the reactor (equilibrium cell) is calculated by the following equations:

$$n_{\text{total}} = n_{\text{cell}} + n_{\text{f}} \quad (1)$$

$$n_{\text{cell}} = \frac{PV_{\text{cell}}}{RT_{\text{cell}}Z_{\text{cell}}} \quad (2)$$

$$n_{\text{f}} = \frac{PV_{\text{f}}}{RT_{\text{a}}Z_{\text{a}}} \quad (3)$$

In Eqs. (1–3), P represents the reactor pressure, V_{cell} stands for the space of the reactor (75 cm³), R indicates the universal gas constant, T_{cell} is the reactor temperature, V_{f} stands

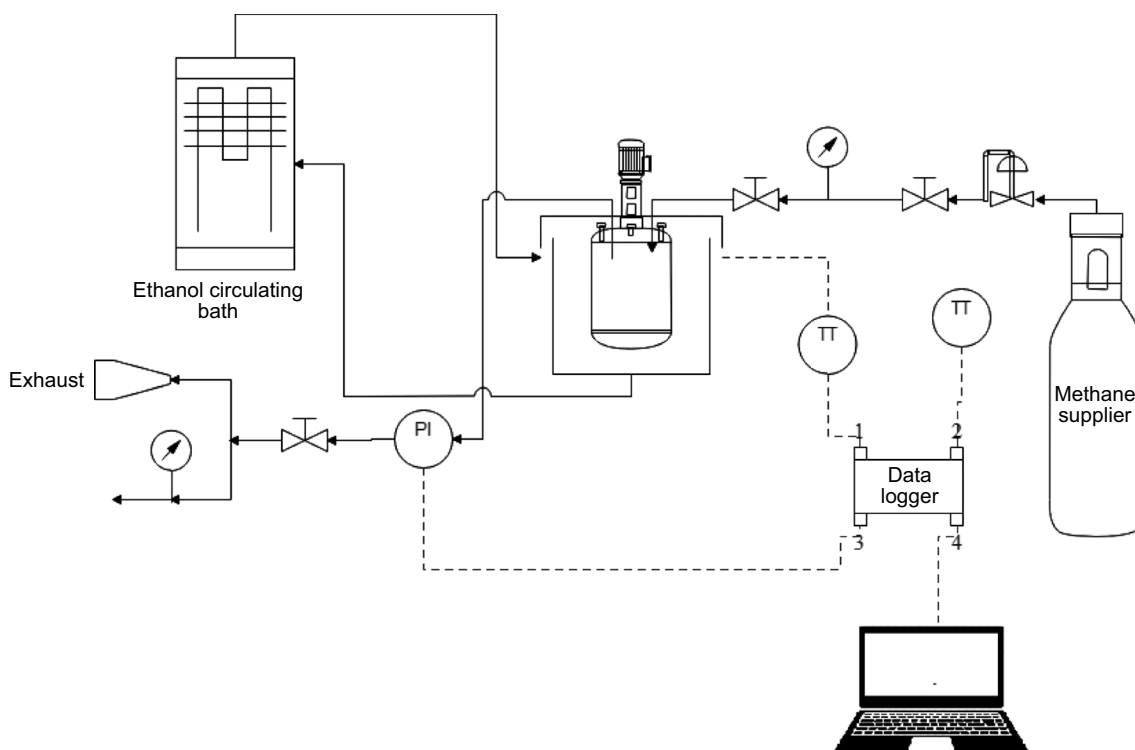


Fig. 1 An overview of the experimental setup, PI and TT are pressure and temperature transmitter, respectively

for the volume of the junctions (15 cm^3), T_a is the ambient temperature, and Z represents the gas compressibility factor computed by the Peng–Robinson equation of state (Peng and Robinson 1976). The amount of gas consumption at time t (trapped gas in hydrate cavities) can be calculated by subtracting the amount of gas at time t in the reactor from the total initial amount of gas fed to the reactor:

$$n_h^t = n_{\text{total}}^0 - n_{\text{total}}^t \quad (4)$$

The gas consumption rate is determined by plotting the diagram of gas consumption versus time. Figure 2 shows the moles of gas consumption at different times.

The initial rate of hydrate formation is evaluated as the slope of the gas consumption versus time plot at the time that the consumption rate increases suddenly (as shown in Fig. 2).

2.3.2 Hydrate stability at atmospheric pressure

After the accomplishment of the gas hydrate formation, the reactor was cooled to 268.15 K over 2.5 h and the system was kept at this temperature for 10 h to gain the stability conditions. Then, by opening the vent valve, the excess gas in the system was removed and the system pressure reached atmospheric pressure. Then, the system was left for 10 h at this temperature to measure the hydrate stability at atmospheric pressure and the change of pressure with the time was

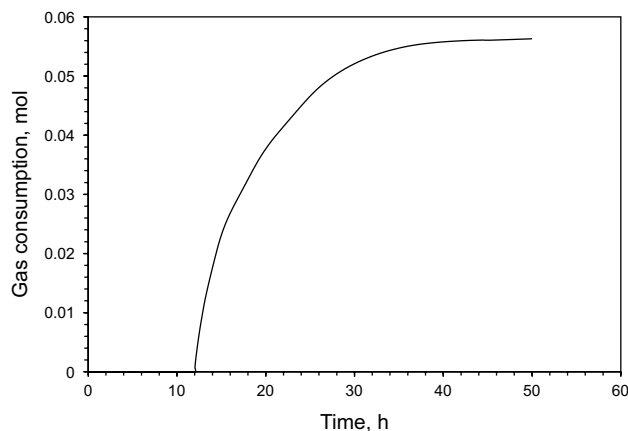


Fig. 2 Gas consumption versus time

recorded for 10 h to analyze the stability of gas hydrates, which were formed in each experiment.

2.3.3 Hydrate storage capacity

After examining/estimating the stability of methane hydrate at atmospheric pressure, the system was warmed up at the slow rate of 1 K h^{-1} to reach ambient temperature ($25 \text{ }^\circ\text{C}$), and by having the knowledge about the final pressure of dissociation and calculating the moles of methane entrapped in

the hydrate cavities, the methane hydrate storage capacity could be calculated. After computing the moles of methane that were entrapped in the gas hydrate lattice, the volume of this amount of methane at standard conditions was calculated (273.15 K, 1 atm). Then, the number of moles of water in 20 cm³ solution was calculated. Then, by having information about the standard molar volume of hydrate for each structure that was reported by Ballard and Sloan (2002), we could calculate the volume of hydrate at standard conditions. For structure I, the standard hydrate molar volume is 22.77 cm³ mol⁻¹. Finally, by dividing the volume of methane to the volume of hydrate, the hydrate storage capacity was computed which is an important parameter in the gas storage and transportation industry.

3 Results and discussion

3.1 Initial rate of hydrate formation

The first parameter that was measured in our experiments was the initial rate of hydrate formation. The assumption is the equality of initial rate of hydrate formation with the rate of gas consumption. Table 2 reports the results for the initial rate of hydrate formation.

We concluded from the results that by increasing the initial pressure, the initial rate of hydrate formation is also increased. The two ILs with imidazolium-based cations lead to an increase in the initial rate of hydrate formation while the ILs with ammonium-based cations decrease the initial rate of hydrate formation. The results show that the ILs with imidazolium-based cations due to their electrostatic charges have a strong synergetic effect on methane hydrate formation and are good choices to use as an aqueous solution to increase the initial rate of methane hydrate formation. On the other hand, the ILs with ammonium-based cations decrease the initial rate of hydrate formation. It is interpreted from the results in Table 2 that the average rates of hydrate formation in the presence of pure water, 1 wt% BMIM-BF₄, 10 wt% BMIM-BF₄, 15 wt% BMIM-BF₄, 20 wt% BMIM-BF₄, 10 wt% BMIM-DCA and 10 wt% TEACl were 0.0556, 0.1087, 0.1263, 0.1535, 0.1667, 0.1362 and 0.0459 mmol min⁻¹, respectively. The comparison between the results shows that 1 wt% BMIM-BF₄, 10 wt% BMIM-BF₄, 15 wt% BMIM-BF₄, 20 wt% BMIM-BF₄ and 10 wt% BMIM-DCA aqueous solutions increase the average rate of hydrate formation by 95.6%, 127.1%, 176.1%, 199.8% and 144.9%, respectively. The 10 wt% TEACl aqueous solution decreases the average rate of hydrate formation by 17.4%. For the same concentration of ILs in the water, 10 wt% BMIM-DCA has more synergetic effect on the average rate of hydrate formation than 10 wt% BMIM-BF₄.

Table 2 Initial rate of methane hydrate formation in various aqueous solutions

Solution	Initial pressure, MPa	Initial rate of methane hydrate formation, mmol min ⁻¹
Pure water	7.0	0.0665
Pure water	6.0	0.0631
Pure water	5.0	0.0526
Pure water	4.6	0.0481
Pure water	4.2	0.0477
1 wt% BMIM-BF ₄	7.0	0.1033
1 wt% BMIM-BF ₄	6.0	0.0988
1 wt% BMIM-BF ₄	5.0	0.1241
10 wt% BMIM-BF ₄	7.0	0.2293
10 wt% BMIM-BF ₄	6.0	0.1242
10 wt% BMIM-BF ₄	6.0	0.1237
10 wt% BMIM-BF ₄	5.8	0.1208
10 wt% BMIM-BF ₄	5.0	0.0922
10 wt% BMIM-BF ₄	5.0	0.1011
10 wt% BMIM-BF ₄	5.0	0.1042
10 wt% BMIM-BF ₄	5.0	0.1148
15 wt% BMIM-BF ₄	6.6	0.2065
15 wt% BMIM-BF ₄	5.7	0.1385
15 wt% BMIM-BF ₄	4.7	0.1073
15 wt% BMIM-BF ₄	3.8	0.1618
20 wt% BMIM-BF ₄	6.5	0.2021
20 wt% BMIM-BF ₄	6.4	0.2137
20 wt% BMIM-BF ₄	6.3	0.2013
20 wt% BMIM-BF ₄	5.8	0.1811
20 wt% BMIM-BF ₄	5.7	0.1836
20 wt% BMIM-BF ₄	5.0	0.1684
20 wt% BMIM-BF ₄	4.7	0.1094
20 wt% BMIM-BF ₄	3.8	0.0740
10 wt% BMIM-DCA	7.0	0.1644
10 wt% BMIM-DCA	6.3	0.1479
10 wt% BMIM-DCA	6.0	0.1419
10 wt% BMIM-DCA	5.6	0.1366
10 wt% BMIM-DCA	5.5	0.1341
10 wt% BMIM-DCA	4.9	0.1261
10 wt% BMIM-DCA	3.5	0.1021
10 wt% TEACl	7.1	0.0576
10 wt% TEACl	6.9	0.0543
10 wt% TEACl	5.9	0.0526
10 wt% TEACl	5.5	0.0511
10 wt% TEACl	4.7	0.0447
10 wt% TEACl	4.6	0.0421
10 wt% TEACl	4.2	0.0404
10 wt% TEACl	4.1	0.0246

The expanded uncertainty U_c is: $U_c(T) = \pm 0.1$ K, $U_c(w) = \pm 0.01$, $U_c(P) = \pm 0.01$ MPa (with 0.95 level of confidence)

3.2 Hydrate stability at atmospheric pressure

After the termination of the hydrate formation step, methane hydrate stability at atmospheric pressure was measured which was the second parameter that was measured in this work. Figure 3 demonstrates methane hydrate dissociation pressure variation with time at an initial pressure of 5.0 MPa

As Fig. 3 shows at the beginning of 10 h, the methane hydrate dissociation curve has a very sharp slope and it becomes a straight line at the end of the time perhaps due to the following reasons:

- (1) The main reason is the self-preservation of hydrate at atmospheric pressure, which remains hydrate metastable below its hydrate formation pressure, and at temperatures below ice formation temperatures. Hydrate dissociation is an endothermic reaction, when a part of the hydrate is dissociated, it absorbed heat from its surrounding and an ice layer is formed around the hydrate, which leads to the prevention of hydrate dissociation. For the self-preservation of hydrate, many mechanisms have been proposed in the literature (Xiao et al. 2018; Lin et al. 2004; Zhong et al. 2016).
- (2) The experiments were carried out as a constant-volume process. After dissociation of a part of the hydrate, the pressure of the vessel was increased, and at higher pressures the dissociation of hydrate was harder than lower pressures.

It is also concluded from the results that all three ILs decrease the stability of methane hydrate. Figure 3 shows that two ILs with imidazolium-based cations decrease

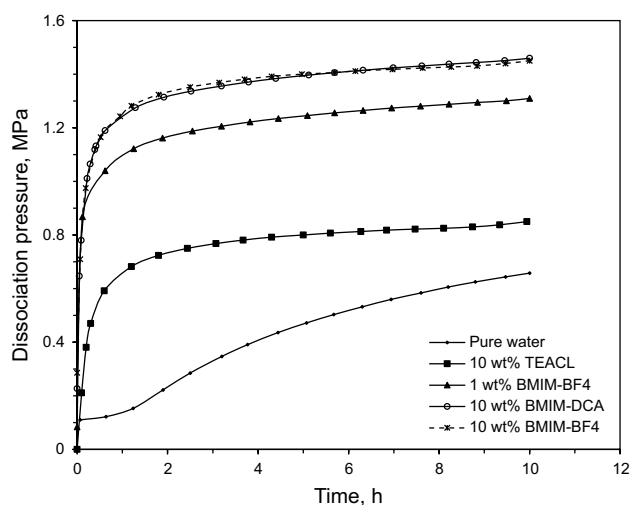


Fig. 3 Methane hydrate dissociation pressure versus time at an initial pressure of 5.0 MPa

Table 3 Methane hydrate dissociation percent after 10 h

Solution	Initial pressure, MPa	Dissociation, %
Pure water	5.0	54.83
1 wt% BMIM-BF ₄	5.0	68.95
10 wt% BMIM-BF ₄	5.0	72.60
10 wt% BMIM-DCA	5.0	63.63
10 wt% TEACL	5.0	53.25
Pure water	6.0	52.30
1 wt% BMIM-BF ₄	6.0	61.74
10 wt% BMIM-BF ₄	6.0	63.20
Pure water	7.0	42.86
1 wt% BMIM-BF ₄	7.0	62.85
10 wt% BMIM-BF ₄	7.0	67.74

The expanded uncertainty U_c is: $U_c(T) = \pm 0.1$ K, $U_c(w) = \pm 0.01$, $U_c(P) = \pm 0.01$ MPa (with 0.95 level of confidence)

methane hydrate stability more than the IL with ammonium-based cations.

Table 3 shows the dissociation of methane hydrate for various solutions at different initial pressures.

Table 3 indicates that the minimum decomposition rate is for pure water at an initial pressure of 7 MPa and the maximum decomposition rate is for 10 wt% BMIM-BF₄ aqueous solution at an initial pressure of 5 MPa. This means that some stabilizers like starch, hydroxyethyl cellulose (HEC) and nanoparticles must be used to increase the stability of IL solutions.

3.3 Hydrate storage capacity

Gas injection to the cell was stopped after the hydrate was formed and the hydrate storage capacity was calculated using the final moles of methane in the cell. Table 4 shows the methane hydrate storage capacity for different solutions at different initial pressures.

Hydrate storage capacity is one of the most important parameters in the gas storage and transportation industry. The higher the volume of gas in the hydrate, the higher the storage capacity of hydrate. When the hydrate storage capacity increases, the hydrate technology becomes more efficient and economical to use for storage and transportation of gas. Methane hydrate storage capacity increases by increasing the feed pressure. The aforementioned ILs increase the hydrate storage capacity under the same conditions compared to the formation of methane hydrate in the presence of pure water, and the synergetic effects of two ILs with imidazolium-based cations are more than ILs with ammonium-based cations. For an initial pressure of 7 MPa, 10 wt% BMIM-BF₄ and 10 wt% BMIM-DCA aqueous solutions enhance methane

Table 4 Methane hydrate storage capacity

Solution	Initial pressure, MPa	Storage capacity, v/v
Pure water	5.0	36.98
1 wt% BMIM-BF ₄	5.0	47.52
10 wt% BMIM-BF ₄	5.0	57.34
10 wt% BMIM-DCA	5.0	57.20
10 wt% TEACl	5.0	37.80
Pure water	6.0	38.04
1 wt% BMIM-BF ₄	6.0	61.38
10 wt% BMIM-BF ₄	6.0	75.85
10 wt% BMIM-DCA	6.0	71.20
10 wt% TEACl	6.0	49.08
Pure water	7.0	39.14
1 wt% BMIM-BF ₄	7.0	40.31
10 wt% BMIM-BF ₄	7.0	102.42
10 wt% BMIM-DCA	7.0	94.35
10 wt% TEACl	7.0	58.66

The expanded uncertainty U_c is: $U_c(T) = \pm 0.1$ K, $U_c(w) = \pm 0.01$, $U_c(P) = \pm 0.01$ MPa (with 0.95 level of confidence)

hydrate storage capacity by 161.7% and 141.1%, respectively, compared to pure water.

The methane storage capacity in gas hydrate form has been reported by several researchers (Ganji et al. 2007, 2013; Mohammadi et al. 2017; Prasad et al. 2014), which were at different conditions such as different pressures, different temperatures and different concentrations of aqueous solutions. The storage capacity is very sensitivity to these parameters, and comparison of the results with the literature data was not performed in this study.

4 Conclusion

The effects of three ILs on methane hydrate formation rate, hydrate stability at atmospheric pressure and hydrate storage capacity were investigated, and the following conclusions can be obtained:

- (1) The two imidazolium cation-based ILs increase the methane hydrate formation rate while an ammonium cation-based IL decreases the methane hydrate formation rate. Increasing the concentration of BMIM-BF₄ from 1 to 20 wt% results in increasing the initial rate of methane hydrate formation, and the highest synergetic effect is observed when the concentration of BMIM-BF₄ changes from 1 to 10 wt%.
- (2) All three ILs decrease the methane hydrate stability at atmospheric pressure in comparison with pure water solution. The two ILs with imidazolium-based cations

decrease the methane hydrate stability much more than the ILs with ammonium-based cations. From the aspect of hydrate stability, the best solution is pure water at an initial pressure of 7 MPa.

- (3) All three ILs increase the hydrate storage capacity compared to pure water solution. The two ILs with imidazolium-based cations increase the hydrate storage capacity much more than the ILs with ammonium-based cations. For an initial pressure of 7 MPa, 10 wt% BMIM-BF₄ and 10 wt% BMIM-DCA aqueous solutions enhance methane hydrate storage capacity by 161.7% and 141.1%, respectively, in comparison with pure water.
- (4) By increasing the initial pressure, the hydrate storage capacity is increased.

Acknowledgements The authors wish to acknowledge the Shiraz University of Technology for providing the experimental requirements and computer facilities.

Open Access This article is distributed under the terms of the Creative Commons Attribution 4.0 International License (<http://creativecommons.org/licenses/by/4.0/>), which permits unrestricted use, distribution, and reproduction in any medium, provided you give appropriate credit to the original author(s) and the source, provide a link to the Creative Commons license, and indicate if changes were made.

References

- Ballard AL, Sloan ED. The next generation of hydrate prediction I. Hydrate standard states and incorporation of spectroscopy. *Fluid Phase Equilib.* 2002;194:371–83. [https://doi.org/10.1016/s0378-3812\(01\)00697-5](https://doi.org/10.1016/s0378-3812(01)00697-5).
- Carroll JJ. Natural gas hydrates: a guide for engineers. 1st ed. Boston: Gulf Professional Pub; 2002.
- Carroll JJ. Natural gas hydrates: a guide for engineers. 2nd ed. Boston: Gulf Professional Pub; 2009.
- Del Villano L, Kelland MA. An investigation into the kinetic hydrate inhibitor properties of two imidazolium-based ionic liquids on Structure II gas hydrate. *Chem Eng Sci.* 2010;65:5366–72. <https://doi.org/10.1016/j.ces.2010.06.033>.
- Ganji H, Manteghian M, Omidkhah MR, Mofrad HR. Effect of different surfactants on methane hydrate formation rate, stability and storage capacity. *Fuel.* 2007;86(3):434–41. <https://doi.org/10.1016/j.fuel.2006.07.032>.
- Ganji H, Aalaie J, Boroojerdi SH, Rod AR. Effect of polymer nanocomposites on methane hydrate stability and storage capacity. *J Pet Sci Eng.* 2013;112:32–5. <https://doi.org/10.1016/j.petrol.2013.11.026>.
- Hammerschmidt EG. Formation of gas hydrates in natural gas transmission lines. *Ind Eng Chem.* 1934;26(8):851–5. <https://doi.org/10.1021/ie50296a010>.
- Javanmardi J, Nasrifar Kh, Najibi SH, Moshfeghian M. Economic evaluation of natural gas hydrate as an alternative for natural gas transportation. *Appl Therm Eng.* 2005;25:1708–23. <https://doi.org/10.1016/j.applthermaleng.2004.10.009>.

- Kang SP, Lee H, Lee CS, Sung WM. Hydrate phase equilibria of the guest mixtures containing CO₂, N₂ and tetrahydrofuran. *Fluid Phase Equilib.* 2001;185:101–9. [https://doi.org/10.1016/S0378-3812\(01\)00460-5](https://doi.org/10.1016/S0378-3812(01)00460-5).
- Kang SP, Kim ES, Shin JY, Kim HT, Kang JW, Cha JH, et al. Unusual synergy effect on methane hydrate inhibition when ionic liquid meets polymer. *RSC Adv.* 2013;3:19920–3. <https://doi.org/10.1039/C3RA43891K>.
- Kang SP, Jung T, Lee JW. Macroscopic and spectroscopic identifications of the synergetic inhibition of an ionic liquid on hydrate formations. *Chem Eng Sci.* 2016;143:270–5. <https://doi.org/10.1016/j.ces.2016.01.009>.
- Karaaslan U, Parlaktuna M. PEO—a new hydrate inhibitor polymer. *Energy Fuels.* 2002;16(6):1387–91. <https://doi.org/10.1021/ef0200222>.
- Kim KS, Kang JW, Kang SP. Tuning ionic liquids for hydrate inhibition. *Chem Commun.* 2011;47:6341–3. <https://doi.org/10.1039/C0CC05676F>.
- Koh CA, Westcott RE, Zhang W, Hirachand K, Creek JL, Soper AK. Mechanisms of gas hydrate formation and inhibition. *Fluid Phase Equilib.* 2002;194:143–51. [https://doi.org/10.1016/S0378-3812\(01\)00660-4](https://doi.org/10.1016/S0378-3812(01)00660-4).
- Koh CA, Sloan ED, Sum AK, Wu DT. Fundamentals and applications of gas hydrates. *Annu Rev Chem Biomol Eng.* 2011;2:237–57. <https://doi.org/10.1146/annurev-chembioeng-061010-114152>.
- Lederhos JP, Longs JP, Sum A, Christiansen RI, Sloan ED. Effective kinetic inhibitors for natural gas hydrates. *Chem Eng Sci.* 1996;51:1221–9. [https://doi.org/10.1016/0009-2509\(95\)00370-3](https://doi.org/10.1016/0009-2509(95)00370-3).
- Lee W, Shin JY, Cha JH, Kim KS, Kang SP. Inhibition effect of ionic liquids and their mixtures with poly(*N*-vinylcaprolactam) on methane hydrate formation. *J Ind Eng Chem.* 2016a;38:211–6. <https://doi.org/10.1016/j.jiec.2016.05.007>.
- Lee W, Shin JY, Kim KS, Kang SP. Kinetic promotion and inhibition of methane hydrate formation by morpholinium ionic liquids with chloride and tetrafluoroborate anions. *Energy Fuels.* 2016b;30:3879–85. <https://doi.org/10.1021/acs.energyfuels.6b00271>.
- Lee W, Shin JY, Kim KS, Kang SP. Synergetic effect of ionic liquids on the kinetic inhibition performance of poly(*N*-vinylcaprolactam) for natural gas hydrate formation. *Energy Fuels.* 2016c;30:9162–9. <https://doi.org/10.1021/acs.energyfuels.6b01830>.
- Li KN, Tong MW, Lin K. Experimental research on the influence of jet pump on the cooling storage property of gas hydrates. *Int J Mod Phys B.* 2005;19:507–9. <https://doi.org/10.1142/S021797920502892X>.
- Lin W, Chen GJ, Sun CY, Guo XQ, Wu ZK, Liang MY, et al. Effect of surfactant on the formation and dissociation kinetic behavior of methane hydrate. *Chem Eng Sci.* 2004;59(21):4449–55. <https://doi.org/10.1016/j.ces.2004.07.010>.
- Mohammadi A, Manteghian M, Mohammadi AH, Jahangiri A. Induction time, storage capacity, and rate of methane hydrate formation in the presence of SDS and silver nanoparticles. *Chem Eng Commun.* 2017;204(12):1420–7. <https://doi.org/10.1080/00986445.2017.1366903>.
- Nazari K, Moradi MR, Ahmadi AN. Kinetic modeling of methane hydrate formation in the presence of low-dosage water-soluble ionic liquids. *Chem Eng Technol.* 2013;36:1915–23. <https://doi.org/10.1002/ceat.201300285>.
- Peng DY, Robinson DB. A new two-constant equation of state. *Ind Eng Chem Fund.* 1976;15(1):59–64. <https://doi.org/10.1021/i160057a011>.
- Prasad PS, Sowjanya Y, Dhanunjana Chari V. Enhancement in methane storage capacity in gas hydrates formed in hollow silica. *J Phys Chem C.* 2014;118(15):7759–64. <https://doi.org/10.1021/jp411873m>.
- Qureshi MF, Atilhan M, Altamash T, Tariq M, Khraisheh M, Aparicio S, et al. Gas hydrate prevention and flow assurance by using mixtures of ionic liquids and synergistic compounds: combined kinetics and thermodynamic approach. *Energy Fuels.* 2016;30:3541–8. <https://doi.org/10.1021/acs.energyfuels.5b03001>.
- Rasoolzadeh A, Javanmardi J, Eslamimanesh A, Mohammadi AH. Experimental study and modeling of methane hydrate formation induction time in the presence of ionic liquids. *J Mol Liq.* 2016;221:149–55. <https://doi.org/10.1016/j.molliq.2016.05.016>.
- Richard AR, Adidharma H. The performance of ionic liquids and their mixtures in inhibiting methane hydrate formation. *Chem Eng Sci.* 2013;87:270–6. <https://doi.org/10.1016/j.ces.2012.10.021>.
- Seo Y, Kang SP. Enhancing CO₂ separation for pre-combustion capture with hydrate formation in silica gel pore structure. *Chem Eng J.* 2010;161:308–12. <https://doi.org/10.1016/j.cej.2010.04.032>.
- Sloan ED. Fundamental principles and applications of natural gas hydrates. *Nature.* 2003;426:353–63. <https://doi.org/10.1038/nature02135>.
- Sloan ED, Koh CA. Clathrate hydrates of natural gases. 3rd ed. Boca Raton: CRC Press, Taylor and Francis Group; 2008.
- Sugahara T, Murayama S, Hashimoto S, Ohgaki K. Phase equilibria for H₂+CO₂+H₂O system containing gas hydrates. *Fluid Phase Equilib.* 2005;233(2):190–3. <https://doi.org/10.1016/j.fluid.2005.05.006>.
- Sun Z, Wang R, Ma R, Guo K, Fan Sh. Natural gas storage in hydrates with the presence of promoters. *Energy Convers Manag.* 2003;44(17):2733–42. [https://doi.org/10.1016/S0196-8904\(03\)00048-7](https://doi.org/10.1016/S0196-8904(03)00048-7).
- Tariq M, Rooney D, Othman E, Aparicio S, Atilhan M, Khraisheh M. Gas hydrate inhibition: a review of the role of ionic liquids. *Ind Eng Chem Res.* 2014;53:17855–68. <https://doi.org/10.1021/ie503559k>.
- Uchida T, Ikeda IY, Kamata SY, Ohmura R, Nagao J, Zatspeina OY, et al. Kinetics and stability of CH₄-CO₂ mixed gas hydrates during formation and long-term storage. *Chem Phys Chem.* 2005;6(4):646–54. <https://doi.org/10.1002/cphc.200400364>.
- Wasserscheid P, Welton T. Ionic liquids in synthesis. 2nd ed. Hoboken: WILEY-VCH Verlag GmbH & Co. KGaA; 2008.
- Xiao C, Adidharma H. Dual function inhibitors for methane hydrate. *Chem Eng Sci.* 2009;64:1522–7. <https://doi.org/10.1016/j.ces.2008.12.031>.
- Xiao C, Wibisono N, Adidharma H. Dialkylimidazolium halide ionic liquids as dual function inhibitors for methane hydrate. *Chem Eng Sci.* 2010;65:3080–7. <https://doi.org/10.1016/j.ces.2010.01.033>.
- Xiao P, Yang XM, Sun CY, Cui JL, Li N, Chen GJ. Enhancing methane hydrate formation in bulk water using vertical reciprocating impact. *Chem Eng J.* 2018;336:649–58. <https://doi.org/10.1016/j.cej.2017.12.020>.
- Zare M, Haghtalab A, Ahmadi AN, Nazari K, Mehdizadeh A. Effect of imidazolium based ionic liquids and ethylene glycol monoethyl ether solutions on the kinetic of methane hydrate formation. *J Mol Liq.* 2015;204:236–42. <https://doi.org/10.1016/j.molliq.2015.01.034>.
- Zhang J, Yedlapalli P, Lee JW. Thermodynamic analysis of hydrate-based pre-combustion capture of CO₂. *Chem Eng Sci.* 2009;64(22):4732–6. <https://doi.org/10.1016/j.ces.2009.04.041>.
- Zhong JR, Zeng XY, Zhou FH, Ran QD, Sun CY, Zhong RQ, et al. Self-preservation and structural transition of gas hydrates during dissociation below the ice point: an in situ study using Raman spectroscopy. *Sci Rep.* 2016;6:38855. <https://doi.org/10.1038/srep38855>.